(28) R. Prins and J. D. W. van Voorst, *Chem. Phys. Lett.*, **1**, 54 (1967).
(29) A. K. Gregson and S. Mitra, *Chem. Phys. Lett.*, **3**, 392 (1969).
(30) A. K. Gregson and S. Mitra, *Chem. Phys. Lett.*, **3**, 528 (1969).
(31) B. N. Figgis, M. Gerloch, and J. Lewis, *J. Chem. Soc. A*, 2028 (1968).
(32) E. Konig and R. Schnakig, *Theor. Chim. Acta*, **30**, 205 (1973).
(33) A similar approach has been used by Lever and co-workers for other d-electron configurations and symmetries (J. C. Donini, B. R. Hollebone, and A. B. P Lever, *J. Am. Chem. Soc.*, **93**, 6455 (1971)).
(34) M. Gerloch and R. F. McMeeking, *J. Chem. Soc., Dalton Trans.*, 2443 (1976).
(35) This operator should not be confused with the numerical harmonic Hamiltonian used by Lever and co-workers (*Prog. Inorg. Chem.*, **22**, 225 (1977)). Here each spherical harmonic is "normalized" and the operator is used as described in ref 34.
(36) D. M. Brink and G. R. Satchlet, "Angular Momenta", Oxford University Press London, 1968.
(37) C. W. Neilson and G. F. Koster, "Spectroscopic Coefficients for the $p^n$, $d^n$ and $f^n$ Configurations", MIT Press, Cambridge, Mass., 1963.
(38) J. S. Griffith, "The Theory of Transition Metal Ions", Cambridge University Press, New York, N.Y., 1964.
(39) Griffith[38] presents equations for the O* double group which can be applied to both integral and half-integral $J$ values. We have written programs which generate equations, in numerical form, for a number of point groups for any required $J$ value. Only integral $J$ values are required for even-electron systems. The maximum $J$ value required for $d^n$ systems is $^{13}/_2$.
(40) Comparative computational times for the diagonalization of the ligand field matrices, with interelectronic repulsion and nonzero spin–orbit coupling, and calculation of the magnetic properties of symmetry-adapted and non-symmetry-adapted basis sets were performed on the ANU computer center UNIVAC 1100/42.
(41) There is in fact a line of fit near the "triple" cross region (see Figure 5c). The spread is, however, not much. One can get perhaps a similar fit by a slightly different choice of electron-repulsion parameters, but any large variation in the parameters may not be possible. What is important is to have a juxtaposition of $^3A_2$, $^3B_2$, and $^3E$ to have $^3E$ as a mixture of essentially two different configurations.
(42) W. C. Lin, *Inorg. Chem.*, **15**, 1114 (1976).
(43) B. W. Dale, *Mol. Phys.*, **28**, 503 (1974).
(44) M. J. Stillman and A. J. Thomson, *J. Chem. Soc., Faraday Trans. 2*, **70**, 790 (1974).
(45) J. M. Robertson, *J. Chem. Soc.*, 615 (1935); 219 (1977).
(46) G. Lang, K. Spartalian, C. A. Reed, and J. P. Collman, *J. Chem. Phys.*, **69**, 5424 (1978).

Contribution from the Department of Hydrocarbon Chemistry, Faculty of Engineering, Kyoto University, Kyoto 606, Japan

# An MO Theoretical Study on the Dications of Tetrasulfur, Tetraselenium, and Tetratellurium

KAZUYOSHI TANAKA, TOKIO YAMABE, HIROYUKI TERAMA-E, and KENICHI FUKUI*

*Received February 5, 1979*

The electronic structures and the singlet transition energies of the title compounds are studied by using semiempirical INDO-type ASMO–SCF calculations. Localized MO's of each species evaluated from the canonical MO's are also examined. According to the results, these species are all of $6\pi$ Hückel systems, and their characteristic absorptions at the visible region can be assigned as the highest occupied MO ($\pi$) → the lowest unoccupied MO ($\pi^*$) transitions. The electronic structures of $Te_4^{2+}$ are rather different from those of $S_4^{2+}$ and $Se_4^{2+}$ because of the degrees of the contributions from s AO's to the interatomic bonds.

## Introduction

Recent progress in chemistry and physics of the molecular aggregates including chalcogen atoms has had incessant impacts in the field of solid-state science. For instance, polymeric sulfur nitride $(SN)_x$ is a low-dimensional metallic conductor[1] and even becomes a superconductor at 0.3 K,[2] while amorphous chalcogenide glasses consisting of $As_2S_3$ or $As_2Se_3$ have prominent electronic functions available for switching, memory, and imaging devices.[3] Along with the developments of the experimental works, the molecular orbital (MO) theoretical investigations of the electronic structures of these compounds have also been accumulated to reveal their characteristics.[4,5]

Meanwhile, the nature of the chalcogen molecules has gradually become one of the foci of current interest of electronic materials. For example, *cyclo*-octasulfur $S_8$ and *cyclo*-octaselenium $Se_8$ being of crown-shaped rings[6] have been studied by UV and X-ray photoemission spectroscopies and compared with the results of the extended-Hückel and the CNDO/S MO treatments.[7] Sulfur–nitrogen compounds also belong to this group, and disulfur dinitride, $S_2N_2$, and tetrasulfur tetranitride, $S_4N_4$, which are the precursors of $(SN)_x$, have been extensively studied from both experimental[8] and theoretical viewpoints.[9]

On the other hand, over these 150 years, it has been known that the elements sulfur, selenium, and tellurium give various intensely colored solutions in strong acids such as sulfuric acid oleum.[10] A series of recent experimental works has succeeded in determining the nature of these colored species.[11] Namely, they are all polyatomic cations of general formula $X_n^{2+}$ ($S_4^{2+}$, $S_8^{2+}$, $S_{16}^{2+}$, $Se_4^{2+}$, $Se_8^{2+}$, $Te_4^{2+}$, and so on), whose characteristic absorption spectra in the near-UV and the visible regions have all been measured.[11] The geometric structures of these species have been determined by single-crystal X-ray diffraction data of $S_8^{2+}(AsF_6^-)_2$,[12] $Se_4^{2+}(HS_2O_7^-)_2$,[13] $Se_8^{2+}(AlCl_4^-)_2$,[14] $Te_4^{2+}(AlCl_4^-)_2$, and $Te_4^{2+}(Al_2Cl_7^-)_2$.[15] The structure of $S_4^{2+}$ has recently been determined from the force constant analysis.[16] No structural data of $S_{16}^{2+}$ are available at present. The homonuclear groupings of the transition metals are well-known in the "cluster" compounds having ligands attached to the metal cluster, for instance, $[Mo_6Cl_8]^{4+}$. In the nonmetal cations like the present $X_n^{2+}$, lone pairs of electrons take the place of ligands, which suggests an interesting association with the role of the lone pairs in chalcogenide materials.[3b,5c] The structures of $X_8^{2+}$ (X = S or Se) cations are those of folded rings with $C_s$ symmetry,[12,14] and their electronic structures have been investigated on the basis of the MO theoretical treatment by the present authors' group.[17] The geometries of $X_4^{2+}$ (X = S, Se, or Te), however, are all of planar four-membered rings,[13,15,16] like $S_2N_2$[18] as shown in Figure 1. As to the MO theoretical studies on $X_4^{2+}$, there have been only a preliminary work about $Se_4^{2+}$ on the basis of the Hückel MO method[19] and discussions on the geometric structural differences of $S_4^{2+}$, $S_4$, and $S_4^{2-}$ and on the singlet transition energy of $S_4^{2+}$ with the use of the SCF–X$\alpha$–SW method[20] up to now. However, this SCF–X$\alpha$–SW calculation has given a rather poor result, namely, too small transition energy compared with the observed value,[11] which is reminiscent of an underestimation of the interelectron repulsions in the framework of this calculation. In the present paper, we study the electronic structures of $S_4^{2+}$, $Se_4^{2+}$, and $Te_4^{2+}$ systematically on the basis of the MO theoretical treatment. The localized MO's (LMO's) of the species are also probed in order to obtain a quantitative de-

0020-1669/79/1318-3591$01.00/0 

Table I. Slater Exponents ($\zeta_r$) and Valence-State Ionization Potentials ($I_r$) of AO's and Electron Repulsion Integrals[a] for Te

| | $\zeta_r$[b] | $I_r$[c] | (rr\|rr)[d] | (rr'\|rr')[e] |
|---|---|---|---|---|
| 5s | 2.5076 | 20.78 | 11.69 | (5s5p\|5s5p) = 0.523[f] |
| 5p | 2.1617 | 11.04 | 8.46 | (5p5p'\|5p5p') = 0.523 |

[a] The units are shown in eV for $I_r$, (rr|rr), and (rr'|rr'). [b] Reference 23. [c] Reference 24. [d] $(rr|rr) = I_r - E_r$.[21a] $E_r$ denotes the valence-state electron affinity of AO r. For values of $E_r$, see ref 24. [e] Reference 25. [f] Assumed.

Table II. AO Densities,[a] $\pi$-Bond Orders,[b] Atomic Net Charges,[a] and Interatomic Energies ($E_{AB}$)[c] of $X_4^{2+}$

| | $S_4^{2+}$ | $Se_4^{2+}$ | $Te_4^{2+}$ |
|---|---|---|---|
| AO dens s | 1.721 | 1.839 (1.838) | 1.918 (1.918) |
| $p_x$ | 1.140 | 1.080 (1.081) | 1.041 (1.042) |
| $p_y$ | 1.140 | 1.080 (1.082) | 1.040 (1.041) |
| $p_z$ | 1.500 | 1.500 (1.500) | 1.500 (1.500) |
| $\pi$-bond order | 0.500 | 0.500 (0.500) | 0.500 (0.500) |
| atomic net charge | +0.500 | +0.501 (+0.499) | +0.501 (+0.499) |
| $E_{AB}$ $X_1$-$X_2$ | −16.424 | −13.747 | −10.518 |
| $X_1$-$X_4$ | −16.424 | −13.851 | −10.349 |

[a] The values on $X_1$ or $X_3$. Values in parentheses are those on $X_2$ or $X_4$. [b] The values between $X_1$ and $X_2$. Values in parentheses are those between $X_1$ and $X_4$. [c] The units are shown in eV.

scription of the nature of the bonding and lone pairs. Furthermore, we also try to discuss the singlet transition energies and their assignments for these species to compare with the observed absorption spectra.

## Method of Calculation

The calculations are performed with the use of the semiempirical INDO-type ASMO–SCF method for valence electrons.[21a] This method has afforded fairly reasonable results not only for the transition energies,[21] because of appropriate parametrization for Coulomb repulsion integrals,[22] but also for the shapes of MO's and the electronic structures of $As_4S_6$ and $As_4S_4$[5d] being molecular analogue models in amorphous $As_2S_3$ glass. Parameters adopted for S are the same as those in ref 21a, those for Se are the same as those in ref 9e, and those for Te are listed in Table I. The contributions from d atomic orbitals (AO's) are expected to be small for the present cationic species $X_4^{2+}$. Similar conclusions have been reached on $S_4N_4$, $SO_4^{2-}$, $SF_6$, and various sulfur compounds of different valence states.[26] Hence we exclude the d AO's of S, Se, and Te in the present calculation. The geometries of $X_4^{2+}$ employed are those in Figure 1. Namely, $S_4^{2+}$ is in $D_{4h}$ symmetry,[16] and $Se_4^{2+}$ and $Te_4^{2+}$ are in $C_{2h}$ symmetries being very near $D_{4h}$ structures.[13,15] The LMO's of these species are evaluated from the canonical MO's (CMO's) thus obtained by the transformations under the criterion proposed by Edmiston and Ruedenberg.[27]

## Electronic Structures

The calculated AO densities and the $\pi$-bond orders from the CMO's are listed in Table II along with the interatomic contributions ($E_{AB}$) to the total energy[28] of each species. Negative values of the $E_{AB}$'s mean attractive interactions. The values of $p_z$ AO ($\pi$AO) densities of $S_4^{2+}$, $Se_4^{2+}$, and $Te_4^{2+}$ clearly show that these species are of $6\pi$ aromatic character as has been conjectured for $Se_4^{2+}$ [19] and calculated for $S_4^{2+}$.[20] Thus the $\pi$-bond orders between the adjacent atoms are all 0.5. These $6\pi$ electrons contribute to the stabilization of the square-planar forms, while $14\pi$ electrons in the hypothetical

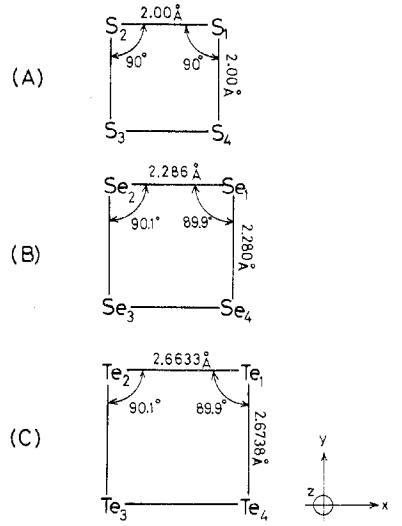


**Figure 1.** Molecular geometries of $S_4^{2+}$ (A), $Se_4^{2+}$ (B), and $Te_4^{2+}$ (C) with coordinate axes employed in the calculation.

octagonal planar forms of $S_8^{2+}$ and $Se_8^{2+}$ occupying almost all of the $\pi^*$ MO's cannot maintain the planar structures.[12,14,17] It is to be noted that the values of s AO densities increase in the order $S_4^{2+} < Se_4^{2+} < Te_4^{2+}$. This means that the participation of s AO's on each atom into the sp hybridization decreases in the order S > Se > Te. These decreasing tendencies are characteristic of atoms having electrons with larger principal quantum numbers.[29]

The $E_{AB}$ values in $X_4^{2+}$ indicate that the Te–Te bond is the weakest of the three species. This weakness of the Te–Te bond is a probable cause of the rapid deformation of $Te_4^{2+}$ into $Te_{2n}^{2n+}$ ($n$ = 1, 3, or 4) in the acid solution[11,30] apart from $S_4^{2+}$ or $Se_4^{2+}$.

Meanwhile, the method of the Edmiston–Ruedenberg LMO's[27] presents us with an alternative way of visualizing the chemical bonds and lone pairs in a chemically graspable manner apart from the usual CMO's. These LMO's are obtained from a unitary transformation from the CMO's so that the sum of the self-repulsion energy within each MO may be maximized. In the process of the calculation, all of these LMO's have been checked by a second-order curvature analysis[31] in order to assure that a true maximum has been obtained for the sum of the self-repulsion energies.

In Tables III–V are listed the AO coefficients of the representative truncated LMO's (TLMO's) thus obtained from the CMO's of $X_4^{2+}$ together with the percent of the s character and the percent of the localization which are defined as

$$\% \text{ s character} = (C_{sAO})^2 / \sum_{\mu}^{\text{on A}} (C_\mu)^2 \times 100$$

$$\% \text{ localization} = \begin{cases} \sum_{\mu}^{\text{on A}} (C_\mu)^2 \times 100 \text{ (for the lone pair on atom A)} \\ \left[ \sum_{\mu}^{\text{on A}} (C_\mu)^2 + \sum_{\nu}^{\text{on B}} (C_\nu)^2 \right] \times 100 \text{ (for the bond between atoms A and B)} \end{cases}$$

Table III. Representative TLMO's in $S_4^{2+}$

| type of LMO | | 3s | $3p_x$ | $3p_y$ | $3p_z$ | % s character | % localizn |
|---|---|---|---|---|---|---|---|
| $S_1$ lone pair | | 0.728 | 0.465 | 0.485 | 0.001 | 54.032 | 98.103 |
| $S_2$ lone pair (I) | | 0.552 | −0.279 | 0.288 | 0.622 | 35.819 | 85.175 |
| $S_1$-$S_2$ $\sigma$ bond | $S_1$ | 0.389 | −0.587 | 0.070 | −0.016 | 30.199 | 99.322 |
| | $S_2$ | 0.332 | 0.617 | 0.036 | −0.021 | 22.413 | |
| $S_2$-$S_3$ $\sigma$ bond | $S_2$ | 0.338 | −0.030 | −0.618 | −0.009 | 22.948 | 99.490 |
| | $S_3$ | 0.337 | −0.029 | 0.619 | −0.004 | 22.775 | |
| $S_1$-$S_4$ bent bond (upper) | $S_1$ | 0.296 | 0.051 | −0.401 | 0.499 | 17.587 | 99.593 |
| | $S_4$ | 0.291 | 0.051 | −0.403 | 0.497 | 16.996 | |

Table IV. Representative TLMO's in $Se_4^{2+}$

| type of LMO | | 4s | $4p_x$ | $4p_y$ | $4p_z$ | % s character | % localizn |
|---|---|---|---|---|---|---|---|
| $Se_2$ lone pair | | 0.866 | −0.346 | 0.353 | ~0 | 75.428 | 99.426 |
| $Se_1$ lone pair (I) | | 0.666 | 0.239 | 0.236 | 0.568 | 50.439 | 87.815 |
| $Se_1$–$Se_2$ σ bond | $Se_1$ | 0.235 | −0.664 | 0.003 | 0.012 | 11.097 | 99.647 |
| | $Se_2$ | 0.286 | 0.647 | 0.018 | 0.012 | 16.348 | |
| $Se_1$–$Se_4$ σ bond | $Se_1$ | 0.237 | −0.003 | −0.665 | 0.010 | 11.285 | 99.696 |
| | $Se_4$ | 0.237 | −0.002 | 0.665 | 0.003 | 11.225 | |
| $Se_2$–$Se_3$ bent bond (upper) | $Se_2$ | 0.207 | −0.018 | −0.453 | 0.498 | 8.629 | 99.540 |
| | $Se_3$ | 0.208 | −0.015 | 0.453 | 0.501 | 8.654 | |

Table V. Representative TLMO's in $Te_4^{2+}$

| type of LMO | | 5s | $5p_x$ | $5p_y$ | $5p_z$ | % s character | % localizn |
|---|---|---|---|---|---|---|---|
| $Te_1$ lone pair | | 0.953 | 0.215 | 0.212 | 0 | 90.878 | 99.989 |
| $Te_1$–$Te_2$ π bond | $Te_1$ | 0 | 0 | 0 | 0.566 | | 96.586 |
| | $Te_2$ | 0 | 0 | 0 | 0.804 | | |
| $Te_2$–$Te_3$–$Te_4$ three-center π bond | $Te_2$ | 0 | 0 | 0 | 0.250 | | |
| | $Te_3$ | 0 | 0 | 0 | 0.859 | | 85.219 |
| | $Te_4$ | 0 | 0 | 0 | 0.223 | | |
| $Te_1$–$Te_2$ σ bond | $Te_1$ | 0.160 | −0.688 | −0.005 | 0 | 5.114 | 99.890 |
| | $Te_2$ | 0.160 | 0.689 | −0.007 | 0 | 5.127 | |
| $Te_2$–$Te_3$ σ bond | $Te_2$ | 0.158 | 0.005 | −0.689 | 0 | 4.988 | 99.889 |
| | $Te_3$ | 0.158 | 0.006 | 0.689 | 0 | 4.975 | |

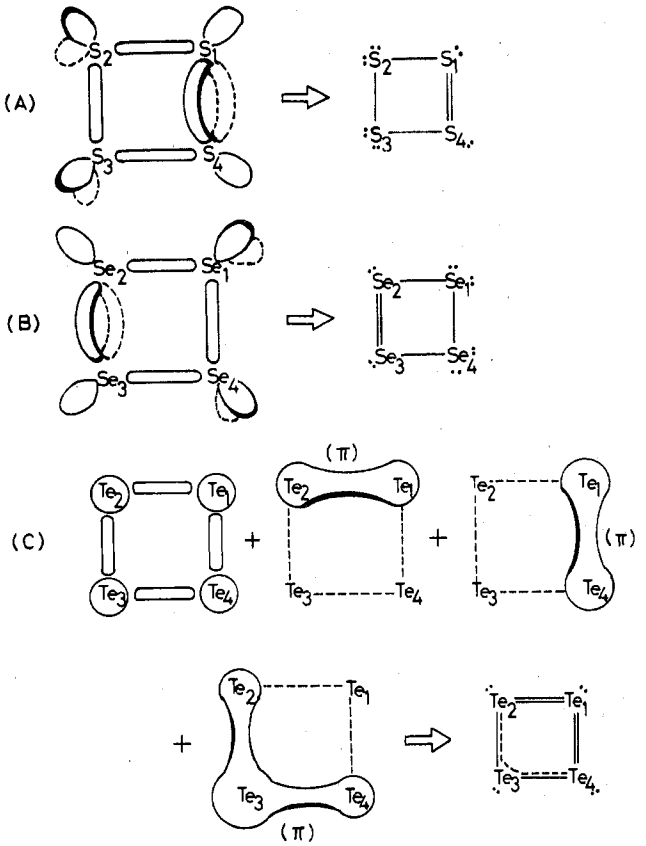


**Figure 2.** Schematic shapes of TLMO's and the valence bond structures of $S_4^{2+}$ (A), $Se_4^{2+}$ (B), and $Te_4^{2+}$ (C). (π) denotes a π-bonding type orbital.

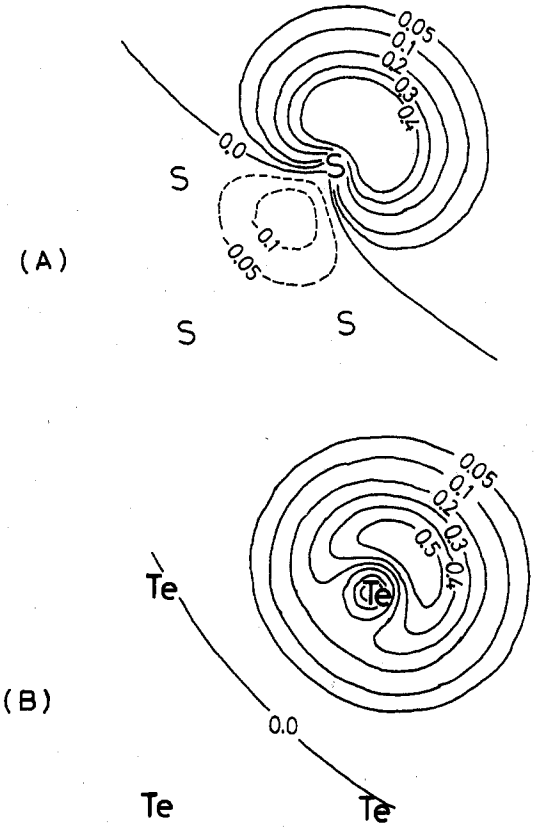


**Figure 3.** Contour plots for the LMO's representing the lone pairs in $S_4^{2+}$ (A) and $Te_4^{2+}$ (B).

In the above formulas, $C_{sAO}$ and $\sum_\mu$ on A signify the LMO coefficient of s AO on atom A and the summation with respect to all AO's on atom A, respectively. The former quantity means the degree of participation of the s AO into the lone pairs or bonds and the latter the degree of localization at the concerned atomic positions of the original LMO.

The schematic shapes of TLMO's and the valence bond structures of $X_4^{2+}$ species are illustrated in Figure 2. In $S_4^{2+}$ there are three σ bonding type orbitals, two bent bond type orbitals, and six lone pair type orbitals. Of these six lone pair orbitals, a set of two lone pairs (I) and (II) is on both $S_2$ and $S_3$ and a lone pair on both $S_1$ and $S_4$. The sets of two lone pairs (I) and (II) are of simply opposite signs of the $p_z$ AO coefficients. These LMO's except lone pairs (I) and (II) are highly localized on the atoms concerned, judging from the percent localization indices. The LMO's in $Se_4^{2+}$ are essentially similar to those in $S_4^{2+}$. In $Te_4^{2+}$ there are four σ bonding type orbitals, two π bonding type orbitals, one three-center π bonding type orbitals being nodeless over three tellurium atoms and four lone pair type orbitals. These LMO's, except the three-center π-type orbital, are highly localized. As a consequence of these types of LMO's in $Te_4^{2+}$, there is also a contribution from the decet structure ($Te_1$) to the valence bond representation apart from $S_4^{2+}$ and $Se_4^{2+}$.

The s character of the lone pairs in $X_4^{2+}$ increases as X changes from S to Te and, accordingly, the s character of the

Table VI. Singlet Transition Energies ($^1\Delta E$)[a] and Oscillator Strengths ($f$) for $S_4^{2+}$, $Se_4^{2+}$, and $Te_4^{2+}$ [b]

| species | $^1\Delta E_{calcd}$ | assignment | $f$ | $^1\Delta E_{obsd}$ |
|---|---|---|---|---|
| $S_4^{2+}$ | 4.393 (3.917) | $E_u\ 1e_g \rightarrow 1b_{1u}$ | 0.769 (0.042) | 3.76 s |
| | (4.696) | $A_{2g}\ 2e_u \rightarrow 3e_u$ | (0) | 4.43 w |
| | (4.828) | $B_{1g}\ 2e_u \rightarrow 3e_u$ | (0) | |
| | (4.931) | $A_{1g}\ 2e_u \rightarrow 3e_u$ | (0) | |
| | 5.055 (5.055) | $B_{1u}\ 2a_{1g} \rightarrow 1b_{1u}$ | 0 (0) | |
| | (5.283) | $B_{2g}\ 2e_u \rightarrow 3e_u$ | (0) | |
| | 5.339 (5.340) | $E_g\ 1e_g \rightarrow 1a_{2g}$ | 0 (0) | |
| $Se_4^{2+}$ | 3.219 (3.065) | $B_u\ 2b_g \rightarrow 2a_u$ | 0.736 (0.493) | 3.02 s |
| | 3.239 (3.090) | $B_u\ 1b_g \rightarrow 2a_u$ | 0.737 (0.495) | |
| | 3.290 (3.228) | $A_u\ 2b_g \rightarrow 5b_u$ | $2.3 \times 10^{-4}$ ($6.0 \times 10^{-4}$) | |
| | 3.312 (3.263) | $A_u\ 1b_g \rightarrow 5b_u$ | 0.017 (0.009) | |
| | 3.334 (3.393) | $A_u\ 2b_g \rightarrow 6b_u$ | 0.017 (0.007) | |
| | 3.368 (3.361) | $A_u\ 1b_g \rightarrow 6b_u$ | $2.3 \times 10^{-4}$ ($7.0 \times 10^{-4}$) | 3.87 w |
| $Te_4^{2+}$ | 2.588 (2.096) | $B_u\ 2b_g \rightarrow 2a_u$ | 0.810 (0.319) | 2.43 s |
| | 2.611 (2.134) | $B_u\ 1b_g \rightarrow 2a_u$ | 0.810 (0.319) | |
| | 2.770 (2.596) | $A_u\ 2b_g \rightarrow 5b_u$ | $2.0 \times 10^{-5}$ (~0) | |
| | 2.806 (2.807) | $A_u\ 1b_g \rightarrow 5b_u$ | 0.007 (0.006) | 2.95 w |
| | 2.854 (2.854) | $A_u\ 2b_g \rightarrow 6b_u$ | 0.007 (~0) | |
| | 2.890 (2.730) | $A_u\ 1b_g \rightarrow 6b_u$ | $2.0 \times 10^{-5}$ (~0) | |

[a] The units are shown in eV. [b] Values in parentheses are those obtained after the CI improvement.

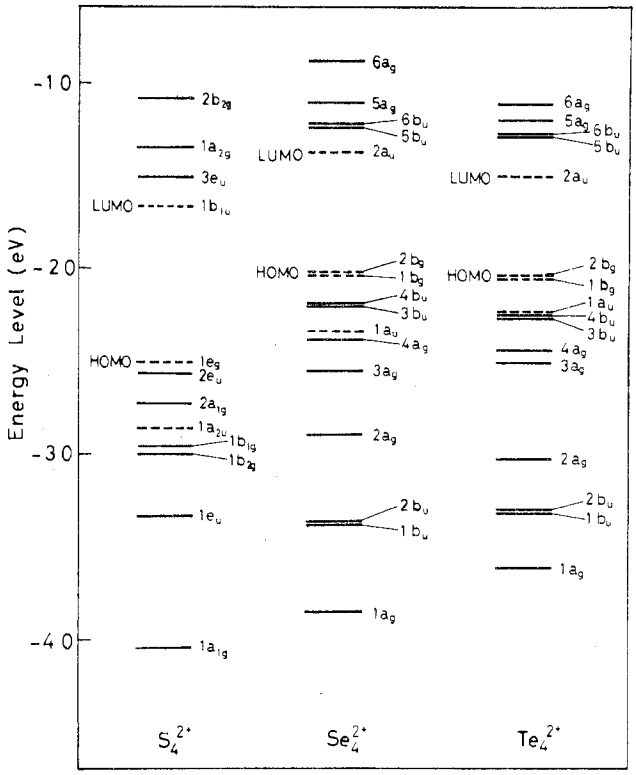


**Figure 4.** Orbital levels of the CMO's of $S_4^{2+}$, $Se_4^{2+}$, and $Te_4^{2+}$. Dashed lines indicate $\pi$ MO's.

$\sigma$ bonds is in the inverse order. Hence lone pairs on $S_1$ and $Te_1$, for instance, are of considerably different shapes, according to the degree of the contributions from s AO's concerned, as shown in Figure 3. These tendencies correspond to what is analyzed as to s AO densities of the CMO's in the above. Owing to appropriate sp hybridizations, there appear a pair of bent bonds in $S_4^{2+}$ and $Se_4^{2+}$ as seen in Figure 2. In $Te_4^{2+}$, however, the $\sigma$ bonds and the $\pi$ bonds do not mingle to form bent bonds because of little participation of five s AO's into the Te–Te bonds.

## Singlet Transition Energies

The calculated singlet transition energies ($^1\Delta E$) and the oscillator strength ($f$) for $X_4^{2+}$ are listed in Table VI. The orbital levels of the CMO's of each species are indicated in Figure 4. These $^1\Delta E$ and $f$ values are further improved by the configuration interaction (CI) method including one-electron excitations within all ranges from the (HO − 4) MO to the (LU + 4) MO (i.e., all unoccupied MO's), where the HOMO and the LUMO denote the highest occupied MO and the lowest unoccupied MO, respectively.

In the case of $S_4^{2+}$, the electronic transitions include $A_{1g} + A_{2g} + B_{1g} + B_{2g}$ ($2e_u \rightarrow 3e_u$) transitions, which should be treated by the CI method, owing to the $D_{4h}$ symmetry. This $A_{2g}$ transition (4.696 eV) is symmetry forbidden but weakly allowed in the $C_{2h}$ case such as $Se_4^{2+}$ or $Te_4^{2+}$. The observed weak absorption at 4.43 eV (280 nm)[11] can be assigned as this transition. The $E_u$ transition ($1e_g \rightarrow 1b_{1u}$) energy, 3.917 eV ($f = 0.042$, after CI), of $S_4^{2+}$ is in reasonable accordance with the observed value 3.76 eV (330 nm) with a strong intensity.[11]

In $Se_4^{2+}$, two $B_u$ transitions ($2b_g \rightarrow 2a_u$ and $1b_g \rightarrow 2a_u$) at 3.065 eV ($f = 0.493$) and 3.090 eV ($f = 0.495$), respectively, well explain the observed strong absorption at 3.02 eV (410 nm).[11] This assignment for $Se_4^{2+}$ has been previously conjectured by the Hückel MO method.[19] The observed weak absorption of $Se_4^{2+}$ at 3.87 eV (320 nm)[11] can be assigned as four weakly allowed $A_u$ transitions ($2b_g \rightarrow 5b_u$, $1b_g \rightarrow 5b_u$, $2b_g \rightarrow 6b_u$, and $1b_g \rightarrow 6b_u$). In $Te_4^{2+}$, two $B_u$ transition energies, 2.096 and 2.134 eV, seem to correspond with the observed strong absorption at 2.43 eV (510 nm).[11] The weak absorption of $Te_4^{2+}$ at 2.95 eV (420 nm)[11] can be assigned as three $A_u$ transitions ($1b_g \rightarrow 5b_u$, $2b_g \rightarrow 6b_u$, and $1b_g \rightarrow 6b_u$) with 2.807, 2.854, and 2.730 eV, respectively.

## Conclusion

We have studied the electronic structures and the transition energies of $S_4^{2+}$, $Se_4^{2+}$, and $Te_4^{2+}$. It has been shown that all of these three species are $6\pi$ Hückel systems. According to the LMO analysis, the lone pairs in $Te_4^{2+}$ almost consist of five s AO's and, consequently, Te–Te bonds almost do not have five s AO components. Further study on the lone pairs in the chalcogen compounds, especially in chalcogenide glass, will be of particular interest.

The calculated results of the singlet transition energies for each species have disclosed that the characteristic intense absorptions at the visible region of these species can be assigned as HOMO $\rightarrow$ LUMO ($\pi \rightarrow \pi^*$) transitions.

**Acknowledgment.** We are grateful to the Data Processing Center of Kyoto University for its generous permission to use the FACOM M190 Computer. We also thank Dr. T. Minato for his help in the MO calculations. This work was supported by a Grant-in-Aid for Scientific Research from the Ministry

of Education of Japan (Grant No. 255315).

**Registry No.** $S_4^{2+}$, 12597-09-0; $Se_4^{2+}$, 12310-32-6; $Te_4^{2+}$, 12597-50-1.

## References and Notes


(1) (a) V. V. Walatka, Jr., M. M. Labes, and J. H. Perlstein, *Phys. Rev. Lett.*, **31**, 1139 (1973); (b) C. Hsu and M. M. Labes, *J. Chem. Phys.*, **61**, 4640 (1974).
(2) R. L. Greene, G. B. Street, and L. J. Suter, *Phys. Rev. Lett.*, **35**, 1799 (1975).
(3) For example, see (a) S. R. Ovshinsky, *J. Non-Cryst. Solids*, **2**, 99 (1970); (b) S. R. Ovshinsky and H. Fritzsche, *IEEE Trans. Electron Devices*, **ed-20**, 91 (1973); (c) S. R. Ovshinsky and K. Sapru, *Amorphous Liq. Semicond., Proc. Int. Conf., 5th*, 447 (1974); (d) S. R. Ovshinsky, *Int. Kongr. Reprogr. Inf., 4th*, 109 (1975).
(4) (a) T. Yamabe, K. Tanaka, A. Imamura, H. Kato, and K. Fukui, *Bull. Chem. Soc. Jpn.*, **50**, 798 (1977); (b) K. Tanaka, T. Yamabe, K. Fukui, A. Imamura, and H. Kato, *Chem. Phys. Lett.*, **53**, 452 (1978), and references therein.
(5) (a) I. Chen, *Phys. Rev. B*, **8**, 1440 (1973); (b) T. Shimizu and N. Ishi, *Phys. Status Solidi B*, **74**, K39 (1976); (c) M. Kastner, D. Adler, and H. Fritzsche, *Phys. Rev. Lett.*, **37**, 1504 (1976); (d) A. Tachibana, T. Yamabe, M. Miyake, K. Tanaka, H. Kato, and K. Fukui, *J. Phys. Chem.*, **82**, 272 (1978).
(6) (a) A. Caron and J. Donohue, *Acta Crystallogr.*, **14**, 548 (1961); (b) P. Unger and P. Cherin in "Physics of Selenium and Tellurium", W. C. Cooper, Ed., Pergamon, Oxford, 1969, p 223.
(7) (a) I. Chen, *Phys. Rev. B*, **2**, 1053, 1060 (1970); 7, 3672 (1973); **11**, 3976 (1975); (b) W. R. Salaneck, N. O. Lipari, A. Paton, R. Zallen, and K. S. Liang, *Phys. Rev. B*, **12**, 1493 (1975); (c) W. R. Salaneck, C. B. Duke, A. Paton, C. Griffiths, and R. C. Keezer, *Phys. Rev. B*, **15**, 1100 (1977).
(8) For example, see (a) J. Sharma, D. S. Downs, Z. Iqbal, and F. J. Owens, *J. Chem. Phys.*, **67**, 3045 (1977); (b) R. D. Smith, *Chem. Phys. Lett.*, **55**, 590 (1978); (c) J. Bojes and T. Chivers, *Inorg. Chem.*, **17**, 318 (1978).
(9) For example, see (a) D. R. Salahub and R. P. Messmer, *J. Chem. Phys.*, **64**, 2039 (1976); (b) W. R. Salaneck, J. W-p. Lin, A. Paton, C. B. Duke, and G. P. Ceasar, *Phys. Rev. B*, **13**, 4517 (1976); (c) T. Yamabe, K. Tanaka, K. Fukui, and H. Kato, *J. Phys. Chem.*, **81**, 727 (1977); (d) J. A. Jafri, M. D. Newton, T. A. Pakkanen, and J. L. Whitten, *J. Chem. Phys.*, **66**, 5167 (1977); (e) K. Tanaka, T. Yamabe, A. Tachibana, H. Kato, and K. Fukui, *J. Phys. Chem.*, **82**, 2121 (1978).
(10) (a) C. F. Bucholz, *Gehlen's Neues J. Chem.*, **3**, 7 (1804); (b) G. Magnus, *Ann. Phys. (Leipzig)*, **10** (2), 491 (1827); **14**, 328 (1828); (c) M. H. Klaproth, *Philos. Mag.*, **1**, 78 (1798).
(11) (a) R. J. Gillespie and J. Passmore, *Acc. Chem. Res.*, **4**, 413 (1971); (b) R. J. Gillespie and J. Passmore, *Adv. Inorg. Chem. Radiochem.*, **17**, 49 (1975), and references therein.
(12) C. G. Davies, R. J. Gillespie, J. J. Park, and J. Passmore, *Inorg. Chem.*, **10**, 2781 (1971).
(13) I. D. Brown, D. B. Crump, and R. J. Gillespie, *Inorg. Chem.*, **10**, 2319 (1971).
(14) (a) R. K. McMullan, D. J. Prince, and J. D. Corbett, *Chem. Commun.*, 1438 (1969); (b) R. K. McMullan, D. J. Prince, and J. D. Corbett, *Inorg. Chem.*, **10**, 1749 (1971).
(15) T. W. Couch, D. A. Lokken, and J. D. Corbett, *Inorg. Chem.*, **11**, 357 (1972).
(16) R. Steudel, *Z. Naturforsch., B*, **30**, 281 (1975).
(17) K. Tanaka, T. Yamabe, H. Terama-e, and K. Fukui, *Nouv. J. Chim.*, **3**, 379 (1979).
(18) A. G. MacDiarmid, C. M. Mikulski, P. J. Russo, M. S. Saran, A. F. Garito, and A. J. Heeger, *J. Chem. Soc., Chem. Commun.*, 476 (1975).
(19) I. D. Brown, D. B. Crump, R. J. Gillespie, and D. P. Santry, *Chem. Commun.*, 853 (1968).
(20) (a) A. E. Foti, V. H. Smith, Jr., and D. R. Salahub, *Chem. Phys. Lett.*, **57**, 33 (1978); (b) D. R. Salahub, A. E. Foti, and V. H. Smith, Jr., *J. Am. Chem. Soc.*, **100**, 7847 (1978).
(21) (a) T. Yonezawa, H. Konishi, and H. Kato, *Bull. Chem. Soc. Jpn.*, **42**, 933 (1969); (b) H. Konishi, H. Kato, and T. Yonezawa, *Theor. Chim. Acta*, **19**, 71 (1970); (c) H. Yamabe, H. Kato, and T. Yonezawa, *Bull. Chem. Soc. Jpn.*, **44**, 22 (1971); (d) H. Yamabe, H. Kato, and T. Yonezawa, *ibid.*, **44**, 611 (1971).
(22) The two-center Coulomb repulsion integrals are calculated by the Ohno approximation (K. Ohno, *Theor. Chim. Acta*, **2**, 219 (1964)), and the one-center exchange integrals are evaluated by the Slater–Condon parameters estimated by Hinze and Jaffé.[25]
(23) E. Clementi, D. L. Raimondi, and W. P. Reinhardt, *J. Chem. Phys.*, **47**, 1300 (1967).
(24) J. Hinze and H. H. Jaffé, *J. Am. Chem. Soc.*, **84**, 540 (1962).
(25) J. Hinze and H. H. Jaffé, *J. Chem. Phys.*, **38**, 1834 (1963).
(26) (a) A. G. Turner and F. S. Mortimer, *Inorg. Chem.*, **5**, 906 (1966); (b) M. S. Gopinathan and M. A. Whitehead, *Can. J. Chem.*, **53**, 1343 (1974); (c) K. H. Johnson, *Adv. Quantum Chem.*, 7, 143 (1973); (d) V. Bonačić-Koutecký and J. I. Musher, *Theor. Chim. Acta*, **33**, 227 (1974).
(27) C. Edmiston and K. Ruedenberg, *Rev. Mod. Phys.*, **35**, 457 (1963).
(28) J. A. Pople, D. P. Santry, and G. A. Segal, *J. Chem. Phys.*, **43**, S129 (1965).
(29) For example, see J. N. Murrell, S. F. A. Kettle, and J. M. Tedder, "Valence Theory", Wiley, London, 1965, p 52.
(30) (a) R. C. Paul, J. K. Puri, and K. C. Malhotra, *Chem. Commun.*, 776 (1970); (b) N. J. Bjerrum, *Inorg. Chem.*, **11**, 2648 (1972).
(31) (a) W. J. Taylor, *J. Chem. Phys.*, **48**, 2385 (1968); (b) E. Switkes, W. N. Lipscomb, and M. D. Newton, *J. Am. Chem. Soc.*, **92**, 3847 (1970).


---

Contribution from the Nuclear Research Centre, Negev, Beer-Sheva, Israel, and The Ben-Gurion University of the Negev, Beer-Sheva, Israel

# Allotropic Transitions of $Mg_2NiH_4$

Z. GAVRA, M. H. MINTZ, G. KIMMEL, and Z. HADARI*

*Received May 2, 1979*

The crystallographic structure and thermal behavior of $Mg_2NiH_4$ have been studied in the temperature range 25–500 °C. Two allotropic forms of this hydride were identified. An orthorhombic structure with $a$ = 11.36 Å, $b$ = 11.16 Å, and $c$ = 9.12 Å ($P222_1$) containing 16 formula units per cell is stable at ambient temperature. This structure transforms at 210–245 °C to a cubic pseudo-$CaF_2$-type structure with $a$ = 6.490 Å and 4 formula units per cell. The allotropic transition is not accompanied by a change in hydrogen composition which remains the same for both structures (under about a 700-torr hydrogen atmosphere). The enthalpy change associated with this transition was estimated to be 0.80 ± 0.05 kcal/mol of $H_2$ (1.60 kcal/mol of $Mg_2NiH_4$).

## Introduction

The intermetallic compound $Mg_2Ni$ reacts readily with hydrogen at about 300 °C and moderate pressures.[1] The product of the reaction is a ternary hydride with the formula $Mg_2NiH_4$.

The high hydrogen weight capacity of this hydride (about 3.6%), its moderate stability, and its fast absorption–desorption kinetics make $Mg_2NiH_4$ an attractive candidate for hydrogen-storage applications. Thus, for example, $Mg_2NiH_4$ has been utilized recently as a hydrogen-storage unit in fuel tanks of Mercedes-Benz hydrogen-powered vehicles.[2,3]

It has been reported[1] that $Mg_2NiH_4$ has a tetragonal structure with $a$ = 6.464 Å and $c$ = 7.033 Å. No information is available concerning the space group and atomic positions of this structure.

During some thermal analyses which we performed on this compound a reversible allotropic phase transition was observed.

A crystallographic study has thus been carried out on the two allotropic forms of the hydride combined with simulta-

*To whom correspondence should be addressed at The Ben-Gurion University of the Negev.

0020-1669/79/1318-3595$01.00/0 